

## **MATERIALS**

All chemicals and reagents were purchased from commercial source and were used without further purification. Water was purified by Millipore system. NMR data were collected on a 400 MHz Variant spectrometer and reference to tetramethylsilane (TMS) as a standard. The absorption spectra were collected on a Beckman Coulter DU640 spectrophotometer (Fullerton, CA, USA). The emission spectra were recorded on a Fluorolog III fluorometer (Horiba Jobin Yvon, Edison, NJ, USA). A VOYAGER DE-PRO Matrix-assisted laser desorption/ionization (MALDI)-mass spectrometry (MS) from Applied Biosystems (AB; Foster City, CA, USA) was used for the MALDI study. It contains a time-of-flight mass analyzer and a nitrogen laser that operates at 337 nm and ionizes sample. The MS function in reflector modes for positive ions were applied. The MALDI-MS spectral data were processed using the Data Explorer software from AB.

## **METHODS**

### **Cell lines**

All cells were grown in RPMI 1640 (Cambrex Bio Science Walkersville Inc., Walkersville, MD) and fetal calf serum (FCS; HyClone, Logan, UT) (10%) plus penicillin-streptomycin (P/S, 1%). All cell lines were cultured at 37°C and 5% CO<sub>2</sub>. Human H929, RPMI-8226, and OPM2 were purchased from ATCC, human LP1 was a generous gift from Dr. P. Leif Bergsagel (Mayo Clinic, Scottsdale, AZ) and mouse 5TGM1-GFP myeloma cells were a generous gift from Dr. G. Mundy, University of Texas, San Antonio, TX.

**Bone marrow and spleen tissues.** All animal studies were conducted under a protocol approved by the Washington University Institutional Animal Care and Use Committee (IACUC). Three weeks post intravenous (i.v.) tail-vein injection of murine 5TGM1-GFP

tumor cells, mice were sacrificed by CO<sub>2</sub> inhalation. Spleen, tibia and femur were dissected and bone marrow was flushed from bone using ice cold PBS and single cell suspension of spleen and bone marrow was prepared by filtering through a 40 µm nylon strainer. Red blood cells were then lysed using Red Blood Cell Lysing Buffer (Sigma-Aldrich) and washed with ice cold PBS. Spleen and bone marrow cells (n=3/group) were subdivided into four groups (10<sup>6</sup> cells per vial) for flow cytometry. Cells were pre-incubated for 3 min on ice with Fc block (CD16/CD32; BD Pharmingen, Franklin Lakes, NJ). Competitor and inhibitor subgroups were pre-treated with LLP2A (1µg/µL) and fimategrast (10 µg/µL) respectively for 30 min. Cells from all subgroups were stained with the following antibodies (BD Pharmingen) or reagents: PE-B220 (RA3-6B2), PE-CD4 (GK1.5), FITC-CD8, PE-Gr1, PE-mac1, and LLP2A-Cy5 for 25 min on ice and washed twice in PBS/1%BSA/1mM MnCl<sub>2</sub> prior to analysis.

### **Xenograft and orthotopic MM mouse model**

C57/KalwRij mice 3-5 weeks old bred in-house from stock obtained from Dr. Claire M. Edwards (Vanderbilt University Medical Center Cancer Biology, Nashville, TN) were subcutaneously injected at the nape of the neck with 5TGM1-GFP tumor cells (10<sup>5</sup> cell, 100 µl) with and without matrigel or with matrigel only for control. Tumors were allowed to grow for 10 days on average. For the i.v. model, C57/KalwRij mice (3-5 weeks old) were intravenously injected at the tail vein with 5TGM1-GFP tumor cells in PBS (10<sup>6</sup> cell, 100 µl) or only PBS for control (n = 3).

### **Serum protein electrophoresis (SPEP)**

Mice were bled by tail grazing at the desired time point. Blood was collected into Microtainer tubes (Becton Dickinson) and centrifuged for 10 min at 2,300g. Sera were diluted 1:2 in normal saline buffer and analyzed by serum protein electrophoresis (SPEP) on a QuickGel Chamber apparatus using pre-casted QuickGels (Helena Laboratories) according to manufacturer's instruction. Densitometric analysis of the SPEP traces was performed using the clinically certified Helena QuickScan 2000 workstation, allowing a precise quantification of the various serum fractions, including the measurements of gamma/albumin ratio.

### **Synthesis and radiolabeling of CB-TE1A1P-PEG<sub>4</sub>-LLP2A (<sup>64</sup>Cu-LLP2A)**

For <sup>64</sup>Cu radiolabeling, Cu-64 chloride (<sup>64</sup>CuCl<sub>2</sub>) (5–10 μL in 0.5 M HCl) was diluted with 0.1 M ammonium acetate buffer (pH 8, 50–100 μL). CB-TE1A1P-LLP2A solution (5 μg) was diluted with acetate buffer, <sup>64</sup>Cu-acetate (185 MBq (5 mCi)) was added, and the mixture was incubated for 5 min at 80–95°C or 45–60 minutes at room temperature. The radiochemical purity for <sup>64</sup>Cu-CB-TE1A1P-LLP2A (<sup>64</sup>Cu-LLP2A) was >95% as determined by radio-high performance liquid chromatography (radio-HPLC) (1).

### **Small animal PET/CT imaging**

Prior to small animal PET/CT imaging, mice were intravenously injected (tail vein) with <sup>64</sup>Cu-LLP2A (0.9 MBq (SA: 37 MBq/μg)). For in vivo blocking studies, an additional group of mice was injected with the radiopharmaceutical premixed with ~200-fold excess of LLP2A to serve as a blocking agent. At 4 h post injection, mice were anaesthetized with 1–2% isoflurane and imaged in a small animal PET/CT Inveon (Siemens Medical Solutions, Knoxville, TN). Static images were collected for 30 min and co-registered using

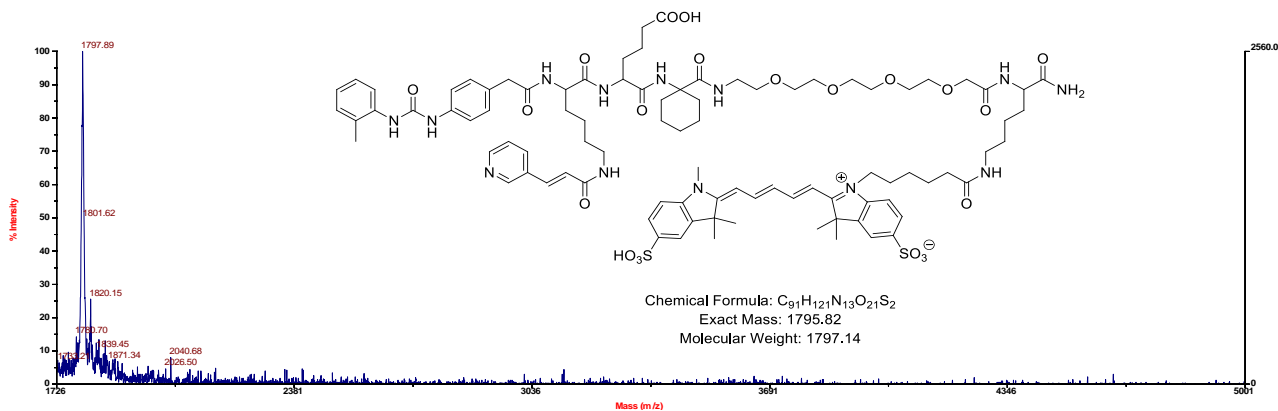
the Inveon Research Workstation (IRW) (Siemens Medical Solutions, Knoxville, TN). Dynamic PET scans were acquired for 0-60 min post intravenous injection of FDG (11 MBq) or  $^{64}\text{Cu}$ -LLP2A (0.9 MBq). PET images were re-constructed with the maximum a posteriori (MAP) algorithm. Analysis of the small animal PET images was done with IRW. Regions of interest (ROI) were selected from PET images using CT anatomical guidelines and the associated activity was quantified. Maximum standard uptake values (SUVs) for both experiments were calculated using  $\text{SUV} = ([\text{nCi/mL}] \times [\text{animal weight (g)}]) / [\text{injected dose (nCi)}]$ . A group of mice was also imaged at 24 h post injection.

### **Flow Cytometry with MM cell lines**

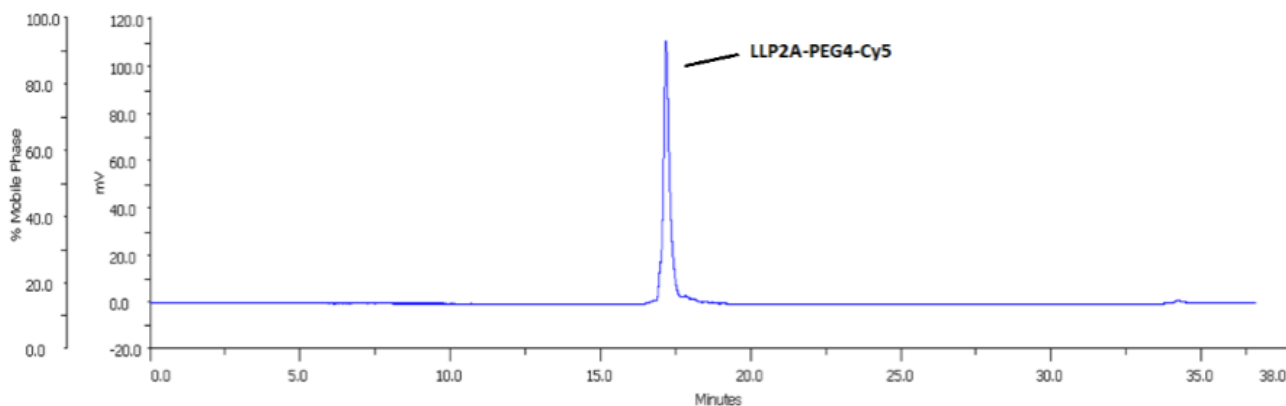
Single cell suspensions of three MM cell lines (human and mouse) were washed three times with PBS and flow buffer (PBS, 0.1% BSA). MM cells ( $10^6$ ) in 0.1 mL of flow buffer were incubated with isotype control antibody or cocktail containing isotype antibody and the LLP2A-Cy5 (5  $\mu\text{l}$  of 1 mg/mL stock in 50  $\mu\text{l}$  Buffer) for 30 min at 4°C in staining buffer (PBS/1% BSA with or without 1 mM  $\text{MnCl}_2$ ). Cells were then washed in the respective buffer three times. Cells were incubated for 30 min with anti-mouse CD49d and IgG2a (BD Pharmingen, USA) for mouse cells and anti-human CD49d and IgG (eBiosciences, USA) for human cells on ice. Finally, after three washes with the respective buffers, cells were analyzed using a FACScan flow cytometer (Becton Dickinson Immunocytometry Systems, Mountain View, California, USA) and the analysis was performed using FlowJo software (Tree Star, San Carlos, CA) gating live cells only.

### **Synthesis of LLP2A-PEG4-Cy5 (LLP2A-Cy5).**

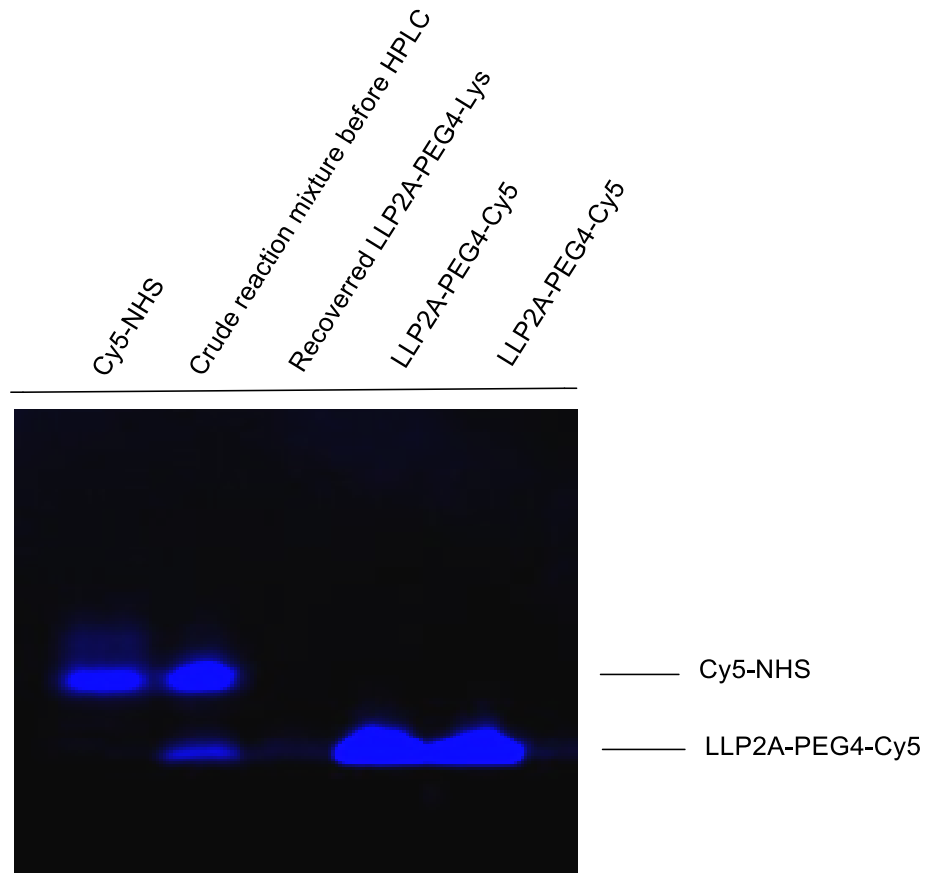
The detailed synthesis of LLP2A is previously described (2). For the synthesis of LLP2A-Cy5, Fmoc-Lys[1-(4,4-dimethyl-2,6-dioxocyclohex-1-ylidene)ethyl] was first coupled to the amino of rink amide MBHA resin. Then, Fmoc was deprotected; PEG4 linker was coupled to the  $\alpha$ -amino of lysine sequentially, followed by assembly of LLP2A. Each coupling reaction was achieved using a 3 or 10 fold excess of amino acid, HOBt and DIC in DMF. The 1-(4, 4-dimethyl-2, 6-dioxocyclohex-1- lidene) ethyl protecting group of the  $\epsilon$ -amino of lysine was removed with 2%  $\text{NH}_2\text{NH}_2$  in DMF. The beads were washed with DMF, MeOH, and DMF, followed by coupling of Sulfo-Cyanine5 NHS ester (a hydrophilic dye, the Ex/Em in DMSO is 646/662 nm). The final product was cleaved off the beads using a mixture of 95% TFA: 2.5% water: 2.5% triisopropylsilane. The crude product was precipitated with cold ether and purified by preparative reversed phase HPLC (C18, 20 X 250 mm, 10  $\mu\text{m}$ ; Waters). Purified LLP2A-PEG4-Cy5 was a dark blue powder after lyophilization in water/acetonitrile mixture. The compound was characterized by analytical HPLC. The purity was determined to be greater than 98% while the overall yield was 20%. The identity of the compounds was confirmed by matrix-assisted laser desorption/ionization time-off light mass spectrometry (MALDI-TOF-MS; MS  $[\text{MH}^+]$ :1797.89; theoretical value: 1795.82).



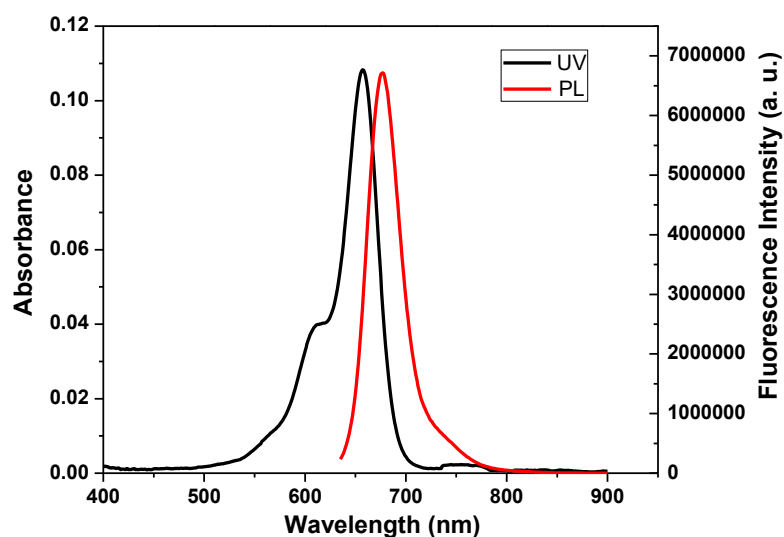
**Supplemental Figure 1:** MALDI of LLP2A-PEG4-Cy5. The compound was mixed with 10 mg/mL  $\alpha$ -Cyano-4-hydroxycinnamic acid (CHCA) matrix in 50% ACN, and 0.1% TFA to give a final concentration of 5 pmol/ $\mu$ L is added to Applied Biosystems (AB) V700666 Sample Plate.



**Supplemental Figure 2:** HPLC (C18, 20 X 250 mm, 10  $\mu$ m; Waters) of purified LLP2A-PEG4-(sulfo-cy5). Using two solvent systems with the gradient elution method at a flow rate of 10 mL/ min. Solvent A was 0.1% TFA in water, and solvent B was 0.1% TFA in acetonitrile. The elution method started with a linear gradient from 10% B over 3 min, followed by 10% to 50% B over 10 min, and stay at 50% B for 5 min, from 50% to 90% B over 10 min. The elution profile was monitored by UV absorbance at 695 nm.



**Supplemental Figure 2a:** SDS-PAGE gel of Cy5-NHS and LLP2A-PEG4-Cy5. LLP2A-PEG4-Cy5 probe in SDS-PAGE is lower than Cy5-NHS due to its interaction with SDS micelles. Since LLP2A-PEG4-Cy5 is the short peptide, a sharp jump in the migration behavior was seen on the gel as a result of the limited and quantized number of SDS micelles bound.



**Supplemental Figure 3:** The absorbance and fluorescence of LLP2A-PEG4-(sulfo-cy5). The Ex/Em= 657/676 nm (in DMSO).

### Staining of primary human tissues with LLP2A-Cy5

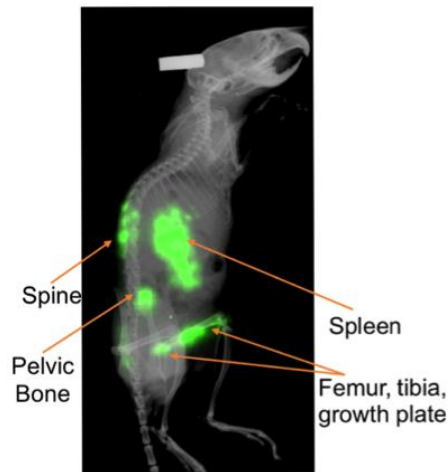
Studies with human samples were approved by the human research protection office at Washington University in St. Louis, and informed consent from the patients was obtained in accordance with the Declaration of Helsinki. Animal studies were approved by the Animal Study Committee at Washington University in St. Louis. De-identified human samples from deceased MM patients were acquired as paraffin sections on slides. Tissue sections were de-paraffinized with Xylene (3 x 10 min) and rehydrated in an ethanol series and water. Sections were then rinsed with PBS/0.1% Triton X100 and blocked with 10% BSA in PBS / 0.1% Triton X100 for 30 minutes, followed by PBS/1 mM MnCl<sub>2</sub> wash. Sections were stained with LLP2A-Cy5 (1/100 dilution, stock 556 μM) and DAPI in PBS/1 mM MnCl<sub>2</sub> for 1 h at room temperature. Sections were then washed with



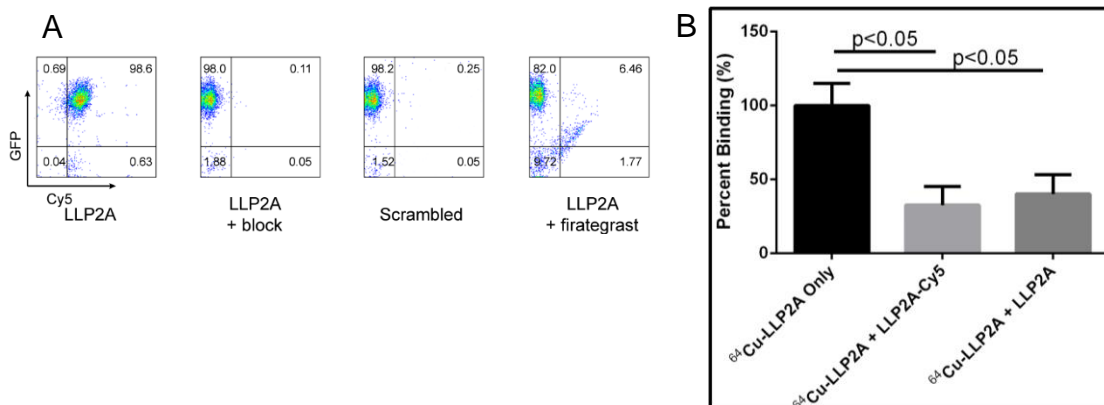
PBS/1 mM MnCl<sub>2</sub> for 1 h in coplin jar on a shaking platform, then rinsed and incubated with 10 mM CuSO<sub>4</sub> pH 5 for 10 min. Tissue sections were finally washed with PBS/1 mM MnCl<sub>2</sub> and coverslips mounted with 70% glycerol containing 2% propyl gallate.

## Human Radiation Dosimetry

The human radiation doses of <sup>64</sup>Cu-LLP2A were estimated for the adult anthropomorphic male model using biodistribution data in BALB/c mice. 5 groups of BALB/c mice (n=5) were injected with 0.78 MBq of the tracer and organs were collected at 1, 2, 4, 12, 24 and 48 h post-injection. The percent injected dose per gram of tissue (%ID/g) was determined by decay correction of the radiopharmaceutical for each sample. The last group of animals was maintained in metabolic cages to collect excreted urine and feces. Time activity curves were created from the collected data expressed in percent of injected dose/activity (%IA). Organ residence times were calculated by integration of the time-data by the trapezoid method assuming no biological clearance beyond the last imaging time point. Residence times were then scaled to human organ weight by the relative to human organ weight method (3). The excreted urine data was fitted with an uptake function ( $f(t)=A_0(1-\exp(-\lambda_{\text{bio}} t))$ ) with  $A_0$  defining the filling fraction and  $\lambda_{\text{bio}}$  the bladder filling time constant. These parameters were used along with the bladder-voiding model in OLINDA to derive bladder and urine excreted residence times. The remainder of the body residence times was defined as the maximum residence time for <sup>64</sup>Cu minus all measured residence times in organs and excretion. Organ residence times were then entered in OLINDA/EXM (4) and human radiation dose were estimated for the adult anthropomorphic male mode.

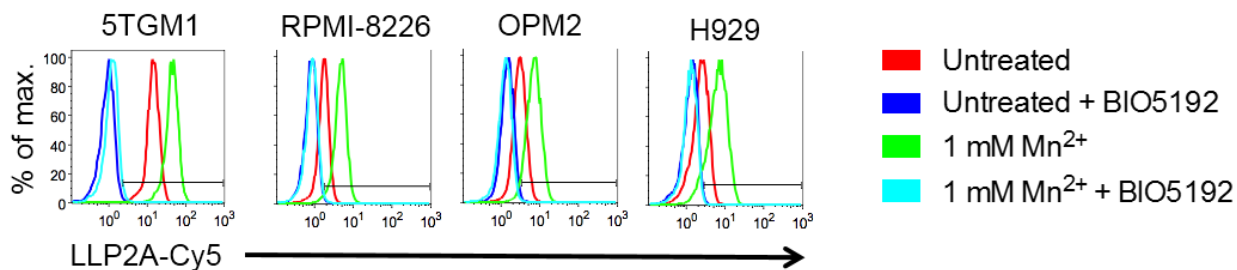


**Supplemental Figure 4:** Optical imaging C57BL/KalwRij 5TGM1-GFP syngeneic metastatic MM model 28 days after intravenous injection of cells. Fluorescence signal (Green) from 5TGM1-GFP cells in the spine, pelvis, femur and spleen can be detected in the living mouse, co-registered with planar X-ray image.

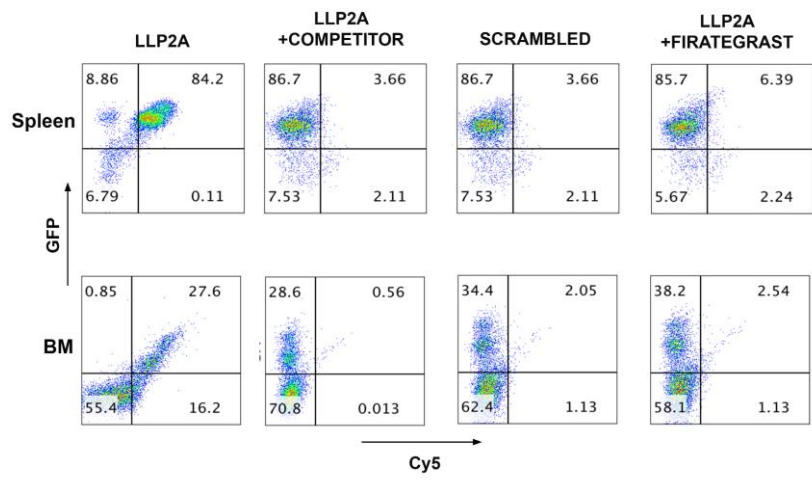


**Supplemental Figure 5:** A. Representative dot blots showing the binding specificity of LLP2A-Cy5 (Cy5 channel) to 5TGM1-GFP cells (n=3/group). The four panels represent the following treatments: 5TGM1 cells + LLP2A-Cy5 only, 5TGM1 cells + Excess LLP2A

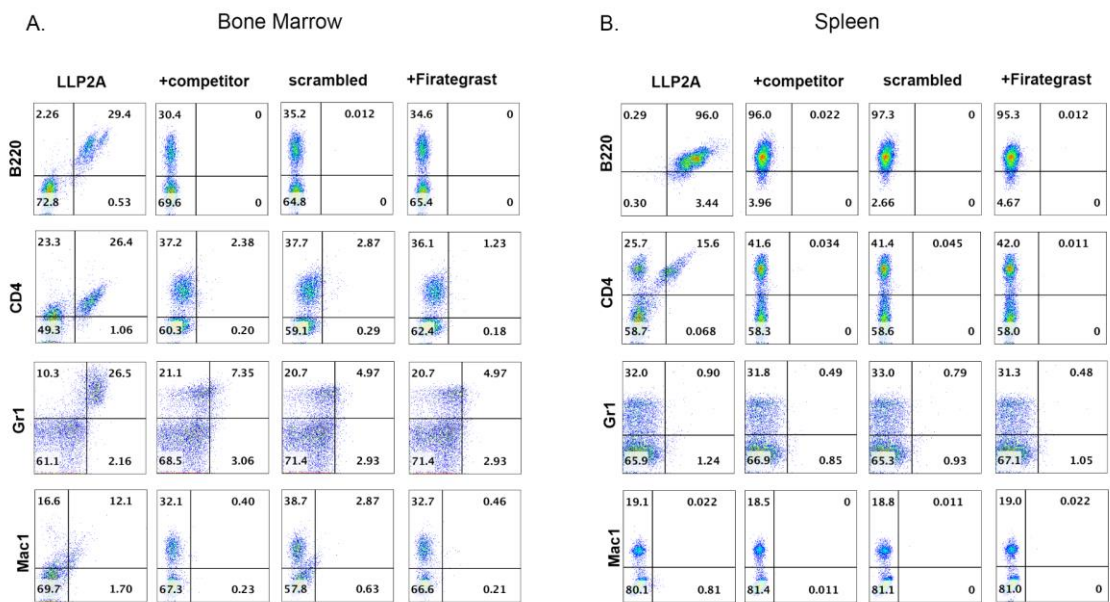
+ LLP2A-Cy5, 5TGM1 cells+ scrambled LLP2A-Cy5, and 5TGM1 cells+ fimategrast + LLP2A-Cy5. B. Percent binding of  $^{64}\text{Cu}$ -LLP2A to 5TGM1 myeloma cells in the presence of 10 fold excess of “LLP2A-Cy5” and “LLP2A only”. Both ligands demonstrated similar blocking effect toward  $^{64}\text{Cu}$ -LLP2A in 5TGM1 myeloma cells.



**Supplemental Figure 6:** Binding of LLP2A-Cy5 to murine (5TGM1) and human (RPMI-8226, OPM2 and H929) myeloma cells. FACS data demonstrates that there is enhanced binding in the presence of manganese ( $\text{Mn}^{2+}$ ). The binding is significantly reduced in the presence of the VLA-4 small molecule inhibitor, BIO5192.



**Supplemental Figure 7.** Representative dot blots showing the ex vivo binding of LLP2A-680 to the B220 positive cells extracted from the BM and spleen of KaLwRij mice bearing iv 5TGM1 tumors (n=3/group).



**Supplemental Figure 8.** Representative dot blots showing the binding of LLP2A-680 to various cell populations extracted from the BM and spleen of KaLwRij mice bearing iv 5TGM1 tumors (n=3/group).

## Supplemental Table 1

Tissue bio-distribution in mice after injection of 0.74 MBq <sup>64</sup>Cu-LLP2A.

Organ	%ID/Gram											
	1 h		2 h		4 h		12 h		24 h		48 h	
blood	1.25	± 0.24	0.57	± 0.12	0.33	± 0.09	0.06	± 0.01	0.02	± 0.00	0.03	± 0.01
lung	4.84	± 0.46	3.67	± 1.02	2.32	± 0.84	0.75	± 0.05	0.32	± 0.02	0.28	± 0.15
liver(all)	3.94	± 0.89	2.33	± 0.68	1.76	± 0.53	0.53	± 0.06	0.48	± 0.06	0.45	± 0.19
spleen	18.34	± 3.48	13.56	± 1.78	10.73	± 3.18	4.44	± 0.69	3.24	± 1.36	3.19	± 1.31
kidney	3.99	± 0.68	2.82	± 0.90	2.93	± 1.20	1.81	± 0.29	2.26	± 0.20	3.08	± 1.23
bladder	184.52	± 145.33	60.32	± 56.62	30.58	± 26.21	0.71	± 0.10	0.26	± 0.10	0.24	± 0.19
gallbladder	2.50	± 1.12	1.37	± 0.49	0.87	± 0.68	0.73	± 0.70	0.29	± 0.31	0.10	± 0.23
muscle	0.75	± 0.09	0.49	± 0.07	0.39	± 0.10	0.12	± 0.02	0.07	± 0.02	0.07	± 0.05
fat	0.50	± 0.25	0.28	± 0.18	0.24	± 0.11	0.10	± 0.04	0.05	± 0.03	0.21	± 0.11
heart	0.64	± 0.13	0.38	± 0.09	0.24	± 0.08	0.10	± 0.03	0.05	± 0.00	0.03	± 0.03
brain	0.08	± 0.02	0.05	± 0.02	0.05	± 0.03	0.02	± 0.01	0.01	± 0.00	0.01	± 0.01
bone	7.91	± 0.57	5.89	± 0.48	5.08	± 1.19	2.47	± 0.58	1.51	± 0.06	1.39	± 0.57
marrow	0.27	± 0.04	0.17	± 0.05	0.15	± 0.07	0.09	± 0.06	0.06	± 0.02	0.05	± 0.03
testes	0.53	± 0.31	0.24	± 0.10	0.18	± 0.10	0.07	± 0.01	0.06	± 0.01	0.07	± 0.03
prostate	3.59	± 4.75	1.12	± 1.01	0.59	± 0.26	0.24	± 0.13	0.20	± 0.08	0.07	± 0.16
adrenals	1.17	± 0.44	0.61	± 0.45	0.58	± 0.28	0.26	± 0.15	0.10	± 0.06	0.77	± 0.78
thyroid	1.56	± 0.39	0.89	± 0.20	0.72	± 0.28	0.39	± 0.12	0.18	± 0.09	0.18	± 0.11
pancreas	1.94	± 1.66	1.31	± 1.42	0.78	± 0.52	0.17	± 0.06	0.20	± 0.07	0.14	± 0.07
thymus	6.18	± 1.58	6.43	± 1.88	6.53	± 2.63	3.34	± 0.11	2.07	± 0.77	2.26	± 1.19
stomach	0.72	± 0.14	0.78	± 0.33	0.58	± 0.19	0.34	± 0.12	0.12	± 0.02	0.14	± 0.08
sm int	3.30	± 0.68	2.33	± 0.54	1.51	± 0.41	0.66	± 0.10	0.41	± 0.07	0.33	± 0.14
u lg int	3.28	± 0.94	2.35	± 0.77	1.49	± 0.44	0.72	± 0.14	0.37	± 0.05	0.43	± 0.20
l lg int	1.77	± 0.55	1.43	± 0.40	1.59	± 0.79	1.18	± 0.51	0.25	± 0.04	1.07	± 0.48

## Supplemental Table 2

Organ residence times of  $^{64}\text{Cu}$ -LLP2A estimated from the mouse bio-distribution data presented in the Supplemental Table 1.

Organ	Residence time (h)
Blood	0.0657 +/- 0.0143
Lungs	0.0738 +/- 0.0175
Liver	0.1129 +/- 0.0276
Spleen	0.0674 +/- 0.0171
Kidney	0.0412 +/- 0.0105
Bladder	0.0541 +/- 0.0451
Gallbladder	0.0004 +/- 0.0003
muscle	0.3354 +/- 0.0706
fat	0.0669 +/- 0.0333
heart	0.0027 +/- 0.0008
Brain	0.0022 +/- 0.0010
Bone	0.0210 +/- 0.0037
marrow	0.0065 +/- 0.0028
testes	0.0003 +/- 0.0001
prostate	0.0006 +/- 0.0005
adrenals	0.0004 +/- 0.0002
thyroid	0.0005 +/- 0.0002
pancreas	0.0025 +/- 0.0018
thymus	0.0045 +/- 0.0013
stomach	0.0031 +/- 0.0011
SMI	0.0370 +/- 0.0083
ULI	0.0122 +/- 0.0034
LLI	0.0097 +/- 0.0040
Heart Content	0.007
Excretion (urine+feces)	13.91
Bladder (MIRD 2hr void)	0.99
Total Measured	0.86
Remainder	3.62

## REFERENCES

1. Beaino W, Anderson CJ. PET imaging of very late antigen-4 in melanoma: comparison of <sup>68</sup>Ga- and <sup>64</sup>Cu-labeled NODAGA and CB-TE1A1P-LLP2A conjugates. *Journal of nuclear medicine : official publication, Society of Nuclear Medicine*. 2014;55:1856-1863.
2. Peng L, Liu R, Andrei M, Xiao W, Lam KS. In vivo optical imaging of human lymphoma xenograft using a library-derived peptidomimetic against alpha4beta1 integrin. *Molecular cancer therapeutics*. 2008;7:432-437.
3. Molina-Trinidad EM, de Murphy CA, Ferro-Flores G, Murphy-Stack E, Jung-Cook H. Radiopharmacokinetic and dosimetric parameters of <sup>188</sup>Re-lanreotide in athymic mice with induced human cancer tumors. *International journal of pharmaceutics*. 2006;310:125-130.
4. Stabin MG, Sparks RB, Crowe E. OLINDA/EXM: the second-generation personal computer software for internal dose assessment in nuclear medicine. *Journal of nuclear medicine : official publication, Society of Nuclear Medicine*. 2005;46:1023-1027.